ACS APPLIED MATERIALS & INTERFACES

Research Article

www.acsami.org

High Capacity and High Density Functional Conductive Polymer and SiO Anode for High-Energy Lithium-Ion Batteries

Hui Zhao,[†,⊥] Neslihan Yuca,[‡,⊥] Ziyan Zheng,[†,§] Yanbao Fu,[†] Vincent S. Battaglia,[†] Guerfi Abdelbast,[∥] Karim Zaghib,[∥] and Gao Liu*[,†]

[†]Environmental Energy Technologies Division, Lawrence Berkeley National Laboratory, Berkeley, California 94720, United States

[‡]Energy Institute, Istanbul Technical University, Istanbul 34469, Turkey

[§]University of California, Berkeley, California 94720, United States

[∥]Institut de Recherche en Électricité d'Hydro-Québec (IREQ), Montreal, Québec H2Z 1A4, Canada

Supporting Information

ABSTRACT: High capacity and high density functional conductive polymer binder/SiO electrodes are fabricated and calendered to various porosities. The effect of calendering is investigated in the reduction of thickness and porosity, as well as the increase of density. SiO particle size remains unchanged after calendering. When compressed to an appropriate density, an improved cycling performance and increased energy density are shown compared to the uncalendered electrode and overcalendered electrode. The calendered electrode has a high-density of ~1.2 g/cm^3. A high loading electrode with an areal capacity of ~3.5 mAh/cm^2 at a C/10 rate is achieved using functional conductive polymer binder and simple and effective calendering method.

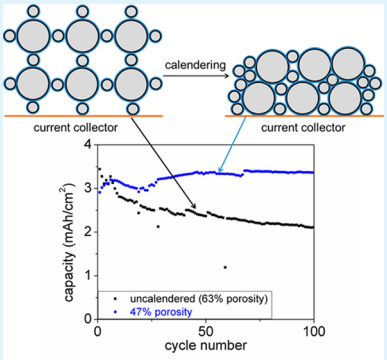

KEYWORDS: *calendering, silicon monoxide, conductive polymer binder, lithium-ion battery*

INTRODUCTION

State-of-the-art lithium-ion technology uses graphite as an anode, with a theoretical gravimetric specific capacity of 372 mAh/g,[1] while the alternative alloy anode materials such as tin (Sn, 994 mAh/g) or silicon (Si, 4200 mAh/g) have much higher gravimetric specific capacities.[2,3] However, almost 300% volume expansion occurs as the material transitions from Si to its fully lithiated phase.[4] Because of this large volume change, the electronic integrity of the composite electrode is disrupted, high and continuous surface side reactions are induced,[5] leading to a drastic capacity decay.[6] Associated with these problems is that most of the current approaches in Si materials research have only achieved an areal capacity of less than 1 mAh/cm^2[2,7] unless electrode architecture designs are integrated into the electrode fabrication process.[8,9]

Instead of merely emphasizing the high specific capacities of Si-containing anode, recent focus in this field is on the fabrication of a thick and high-loading Si-containing electrode with high energy densities.[10] The drastic volume change of pure Si anode poses formidable challenges to build a thick electrode. Also, a high concentration of binder and conductive additive are typically required to achieve a satisfactory cycling performance, these inactive species (binder and carbon black) decrease the electrode level energy density to the extent that makes it less competitive than the state-of-the-art graphite electrode. A well-designed nanostructure was employed to achieve an areal capacity of ~3 mAh/cm^2 at a C/20 rate.[9] However, this nanoarchitecture has a high porosity in the electrode and the electrode density is calculated as ~0.33 g/cm^3. An optimized binder network was applied to a Si/C material and an areal capacity of ~4 mAh/cm^2 was achieved at a C/10 rate, with a calculated electrode density of ~0.62 g/cm^3.[11] A high-density lithium-ion battery leads to a high volumetric energy density, which is especially important for the application in portable electronic devices. The use of Si-containing anode such as Si/C, silicon oxide and silicon-containing alloy have intermediate capacities (800−1500 mAh/g) and volume changes (100−150%); a high-loading electrode is easier to fabricate based on these materials due to the intrinsically smaller volume change. In this work, we demonstrate that by calendering the electrode in to an optimized porosity, the areal capacity of a conductive polymer/SiO electrode is improved by ~1 mAh/cm^2 compared to an uncalendered electrode. A marked areal capacity of ~3.5 mAh/cm^2 is achieved by this simple and effective calendering process, with a high electrode density of ~1.2 g/cm^3.

Received: October 24, 2014
Accepted: December 12, 2014
Published: December 12, 2014

RESULTS AND DISCUSSION

A functional conductive polymer binder, poly(9,9-dioctylfluorene-*co*-fluorenone-*co*-methyl benzoic ester) (PFM, Figure 1a),

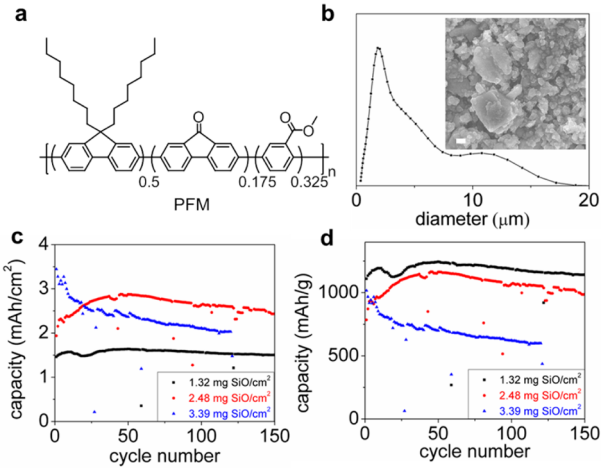

Figure 1. (a) The chemical structure of the PFM binder used in this work. (b) particle size analysis via light scattering for the SiO pristine particles, embedded is the SEM image of the particles with a scale bar of 1 μm. (c) Areal capacity and (d) specific capacity vs cycle no. with increasing loading of the SiO at C/10 (100 mA/g).

was developed by combining adhesion and electrical conduction to provide molecular-level electronic connections between the active material and the conductive polymer matrix.[12−14] Figure 1b shows the characterization of the pristine SiO particles, particle size analysis via light scattering of the particles dispersed in water indicates a bimodal distribution of the particle size, with a smaller particle diameter of ∼1.5 μm, and bigger particle diameter of ∼12 μm. The inset shows the SEM image of the pristine SiO particles, which also reflects this biomodal particle size. We recently established the superior performance of the conductive functional PFM binder/SiO electrode, which only requires 2% (by weight) binder to achieve a stable cycling for ∼500 cycles.[15] To assemble the SiO/PFM electrode with an active material loading as high as ∼3 mg/cm^2, 0.1 g PFM binder is dissolved in 2 g chlorobenzene. 0.9 g SiO particles are then added into the PFM binder solution and the slurry is homogenized for 1 h before lamination. The doctor blade is set to a thickness of 150 μm to coat the electrode laminate.

To showcase the influence of active material loading on the electrochemical performance, three PFM/SiO electrodes are studied with increasing active material loading. All the electrodes investigated in this work contain 90% SiO and 10% PFM binder. Although only 2% binder is necessary for a satisfactory cycling performance in terms of specific capacity, a higher binder loading (10%) could better accommodate the volume change, maintain the electrode integrity and enables a higher loading.[16,17] Also, with an improved mechanical strength provided by the 10% binder loading, the electrode is supposed to better tolerate the calendering process. As shown in Figure 1c,d, the areal-specific capacity is inversely related to the cycling performance. With SiO loadings below 2.5 mg/cm^2, a stable cycling performance with desired specific capacities (>1000 mAh/g) is obtained. As the SiO area loading reaches as high as 3.39 mg/cm^2, the cycling performance exhibits obvious capacity decay. This phenomenon is observed in all lithium-ion battery electrodes, but it is especially pronounced in the Si-based electrodes.[8,18] As the loading and thickness increase, both the ion-transport distance and tortuosity of the pores in the composite electrode increase. Thus, lithium ion diffusion is inhibited. To further increase the areal capacity of the SiO/PFM system, the electrodes with the high loading (∼3 mg SiO/cm^2) are compressed into smaller porosities, as an attempt to increase electronic conductivity and facilitate the lithium ion diffusion by decreasing the ion transport distance.[19−21] As a typical micrometer-size particle-based electrode, the fabricated SiO/PFM has porosities in the range of 60% ∼ 65%. All the porosities were calculated by assuming that the weight fractions and density of each material were not changed by the fabrication process (exact calculation of porosities shown in Supporting Information). During the calendering process, a section of electrode laminate was fed through the gap of the milling machine to compress the electrode to a desired thickness corresponding to the desired electrode porosity.[22] The electrodes are calendered into 51%, 47% and 43% porosities, in order to investigate the relation between porosity and the electrochemical performance.

Figure 2 shows the surface SEM images of pristine and calendered SiO/PFM electrodes. A qualitative examination of

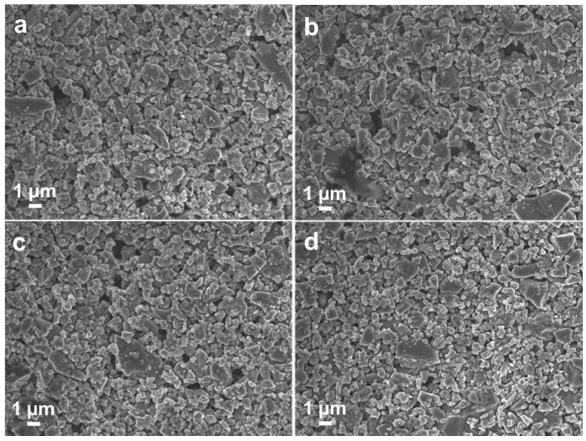

Figure 2. Surface SEM images of (a) uncalendered electrode, (b) calendered to 51% porosity, (c) calendered to 47% porosity, and (d) calendered to 43% porosity.

the particles sizes based on the SEM images indicate that the particles are not broken during the high-pressure calendering process. Also, by comparing Figure 2a (uncalendered, with ∼63% porosity) and Figure 2d (43% porosity), the number of empty spaces (pores) is reduced after calendering. SEM images with different magnifications are shown in Supporting Information Figures S1 and S2, which could further support the unchanged particle sizes and decreased porosities.[23,24] The morphology of the electrodes reveals the fact that we successfully decrease and electrode porosities while maintaining the SiO particles intact, which may lead to an improved electrochemical performance.

Figure 3 shows particle size analysis using a statistic software on the top-view SEM images shown in Figure 2. The material size distribution is measured based on the SEM images of the electrode. More than 100 particles are randomly selected and measured in each figure. The shape of the particles is irregular; therefore, the longest dimension of the particle is used for the statistics. The particle size info further corroborates our

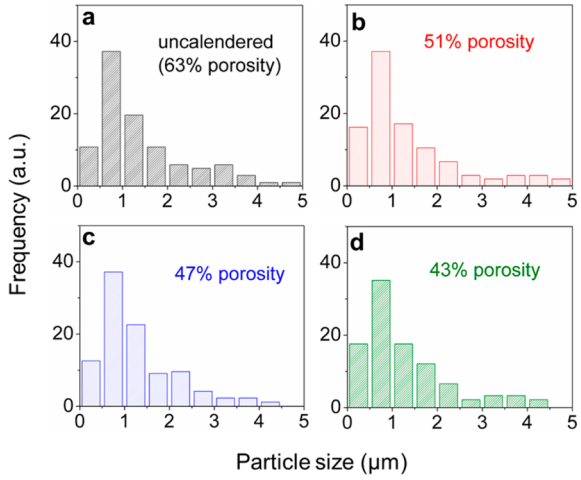

Figure 3. SiO particle size analysis based on the top-view SEM images. (a) Uncalendered electrode. (b) Electrode calendered to 51% porosity. (c) Electrode calendered to 47% porosity. (d) Electrode calendered to 43% porosity.

proposal that particles are barely broken in the high-pressure calendering process. Several other reports observed the fracturing of active materials during calendering.[25] A recent study of the calendering effect on Si alloy/graphite electrode shows that graphite particles allow the Si-containing anodes slide against each other during densification.[26] The SiO anodes in our study have ~10% carbon coating, which may provide a similar smoothing and lubricant effect in the course of calendering. In terms of electrode thickness, the uncalendered electrode with a loading of ~3.0 mg SiO/cm^2 typically has a thickness of ~40 μm, corresponding to a porosity of 63% and an electrode density of 0.83 g/cm^3. When calendered to 30 μm, the laminate has a porosity of 51% and an electrode density of 1.10 g/cm^3; when calendered to 28 μm, the laminate has a porosity of 47% and an electrode density of 1.19 g/cm^3; when calendered to 26 μm, the laminate has a porosity of 43% and an electrode density of 1.28 g/cm^3. Note that the density of our functional conductive polymer/SiO-based electrode is comparable to that of the graphite, while maintaining a high areal capacity of 3.5 mAh/cm^2. Many of previous reported high-loading Si-based electrodes, on the other hand, typically have high porosity and low electrode density.[8,9,11]

The cycling performance with half cell configuration are shown in Figure 4, areal capacities are shown in Figure 4a, and specific capacities are shown in Supporting Information Figure S3. A 47% porosity is determined to deliver the best cell cycling performance, with a high Coulombic efficiency (CE, Figure 4b). Electrodes with 51% porosity may still have too much porosity: the charge transport path is not improved to an ideal case, although the performance is indeed improved compared to the uncalendered electrode. The electrodes with 43% porosity, on the other hand, are overcompressed. The specific capacities (800−1000 mAh/g) of SiO correspond to a volume change of ~100% during lithiation and delithiation. Therefore, moderate high porosity is still necessary on the electrode level to accommodate this large volume change. When overcompressed, the critical connections for electron transport such as particle/binder/particle connection, and binder adhesion on to the particle surface and current collector are also likely to be weakened, and the ion transport pathways become more torturous and narrow to limit fast ion transport. It is likely that

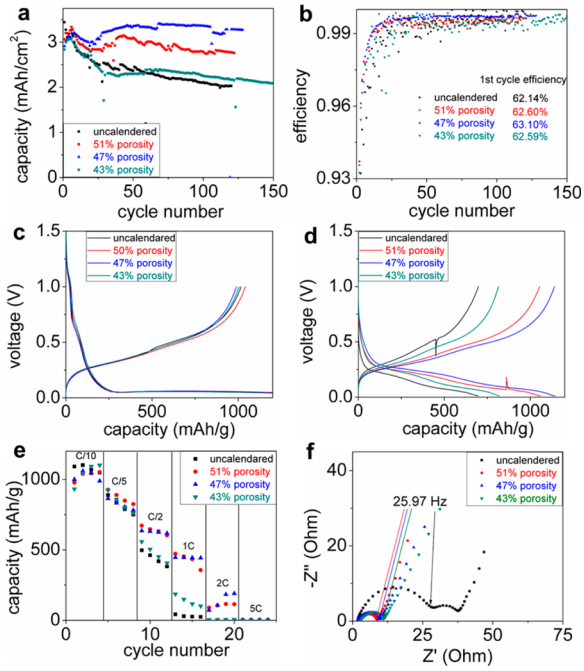

Figure 4. Cycling performance of the SiO/PFM electrode after it was calendered into different porosities. (a) Areal capacity vs cycle number; (b) Coulombic efficiency, the cells were cycled at C/10 (100 mA/g). Voltage profiles of the (c) 1st cycle and (d) 50th cycle. (e) Rate performance and (f) cell impedance based on different porosities.

the particle/binder/particle connection is damaged during overcalendering. Binder adhesion on to the particle surface and current collection are also likely to be affected when too much compression is applied on the electrode. The galvanostatic voltage profiles are shown in Figure 4c (1st cycles) and Figure 4d (50th cycles). The voltage curves basically overlap with each other in the first cycle, indicating that the different electrode porosities do not take effect in the first lithiation/delithiation cycle. However, the voltage curves at the 50th cycle in Figure 4d correlate well with the cycling performance, with 47% porosity showing the lowest overpotential. With 47% porosity, the Coulombic efficiency (CE) of the cell is as high as 99.76% at the 50th cycle, compared to the CEs of electrodes with other porosities (99.33% for uncalendered sample, 99.45% for 51% porosity and 99.45% for 43% porosity, all at 50th cycle). High CE is critical for the long-term stable cycling of the anode electrode and better capacity retention at the full cell level.[27,28] The first cycle CE is typically ~62% (Supporting Information Table S2), which is comparable to most literature reports. Besides the formation of SEI,[29] lithium reacts and converts silicon oxide to silicate, which contributes to the large first cycle irreversible capacity.[30] A prelithiation strategy was used in a previous report to successfully solve this problem.[15] Note that the optimum electrode porosity has an electrode density of ~1.2 g/cm^3 while delivering a high areal capacity of 3.5 mAh/cm^2, which is a high-density electrode compared to most literature reports with similar high loading.

The rate performance at C/2 and 1C rates in Figure 4e reveals that both 47% and 51% porosities improve the electrochemical performance of the SiO/PFM electrode. Either uncalendered electrode (63% porosity) or overcalendered (43% porosity) impairs the rate performance. The impedance of the half cells based on electrodes with different porosities is shown in Figure 4f. The sample cells initially went through a formation

dx.doi.org/10.1021/am507376f | ACS Appl. Mater. Interfaces 2015, 7, 862−866

cycle at C/10, and the impedance was measured at half lithiation, since the voltage of the cell was relatively stable at that stage. The electron conduction of a half cell can be separated into two different ranges. Long-range conduction describes the process where the electrons move from the current collector through the bulk electrode laminate, which is inversely proportional to the high frequency intercept of the impedance sweep. Typically, long-range conductivity corresponding to high frequency impedance is not a limiting parameter for the electrode impedance. Short-range conduction corresponding to low frequency impedance describes the process is a limiting factor, which charge transfer at the electrode/electrolyte interface happens. After it was compressed into more compact electrode architecture, the charge transfer impedance becomes smaller compared to the uncalendered electrodes.

A simplified scheme of the calendering effect on the SiO/PFM electrode is shown in Figure 5. People typically focus on

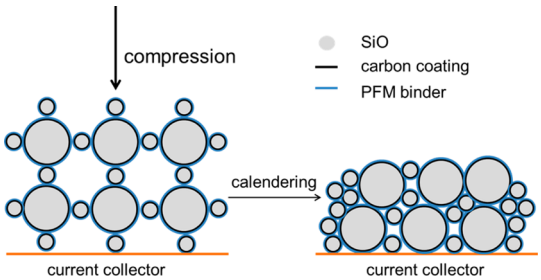

Figure 5. A scheme shows that calendering makes a compact and effective electrode composed of the PFM binder and the bimodal size of carbon-coated SiO particles.

the uncaledered Si-containing electrodes without compressing, there are two reasons for this: first, Si-containing materials are normally brittle and easy to fracture during calendering, particle/active material network tends to be damaged in this process; second, the drastic volume change of Si-containing anode during lithiation and delithiation requires some intrinsic porosities in the electrode laminate to provide a buffering effect. Thus, most previous trials on the calendering of high-capacity alloy anode resulted in a negative effect on the electrochemical performance.[31,32] Two important characters of the SiO pristine particles in this work are proposed to contribute to the well-improved electrochemical performance after calendering: the carbon coating enables the SiO particle slide against each other during compression. Particle locations are able to be rearranged to a compact nature of the electrode without any particle fracture. The bigger particle size (~10 μm) of the SiO anode makes the active material a high tap-density, which facilitates the fabrication of a high-loading electrode.[33] The smaller particles fill out all the void spaces between big particles and helps to build up a continuous conducting network.[11]

CONCLUSIONS

To increase the areal capacity of our functional conductive polymer binder/SiO anodes above the signature 3 mAh/cm^2 without compromising the electrode density, a simple and effective calendering method was used to decrease the electrode porosity and facilitate ion transport. An areal capacity of ~3.5 mAh/cm^2 at a C/10 rate was achieved with 47% porosity and 1.2 g/cm^3 density in the electrode. This high loading electrode with high density is enabled by the dual strategy of utilizing conductive polymer binder and an effective calendering method.

ASSOCIATED CONTENT

Supporting Information

Details about battery assembly and testing, electrochemical data and calculation of electrode porosity and density. This material is available free of charge via the Internet at http://pubs.acs.org.

AUTHOR INFORMATION

Corresponding Author

*Tel.: +1-510-486-7207; fax: +1-510-486-7303; e-mail: gliu@lbl.gov (G. Liu).

Author Contributions

$^{\perp}$These authors contributed equally to this work

Notes

The authors declare no competing financial interest.

ACKNOWLEDGMENTS

This work was funded by the Assistant Secretary for Energy Efficiency, Vehicle Technologies Office of the U.S. Department of Energy (U.S. DOE) under the Batteries for Advanced Transportation Technologies (BATT) Program, which is supported by the U.S. Department of Energy under Contract # DE-AC02-05 CH11231. Neslihan Yuca thanks for the funding provided by The Scientific and Technological Research Council of Turkey (TUBITAK) in Ankara, Turkey.

REFERENCES

(1) Ling, M.; Qiu, J.; Li, S.; Zhao, H.; Liu, G.; Zhang, S. An Environmentally Benign LIB Fabrication Process Using a Low Cost, Water Soluble and Efficient Binder. *J. Mater. Chem. A* **2013**, *1*, 11543−11547.

(2) Boukamp, B. A.; Lesh, G. C.; Huggins, R. A. All-Solid Lithium Electrodes with Mixed-Conductor Matrix. *J. Electrochem. Soc.* **1981**, *128*, 725−729.

(3) Ling, M.; Zhao, H.; Xiao, X.; Shi, F.; Wu, M.; Qiu, J.; Li, S.; Song, X.; Liu, G.; Zhang, S. Low Cost and Environment-benign Crack-Blocking Structure for Long Life and High Power Si Electrodes in Lithium Ion Batteries. *J. Mater. Chem. A* **2015**, Advance Article.

(4) Li, J.; Dahn, J. R. An In Situ X-Ray Diffraction Study of the Reaction of Li with Crystalline Si. *J. Electrochem. Soc.* **2007**, *154*, A156−A161.

(5) Shi, F.; Zhao, H.; Liu, G.; Ross, P. N.; Somorjai, G. A.; Komvopoulos, K. Identification of Diethyl 2,5-Dioxahexane Dicarboxylate and Polyethylene Carbonate as Decomposition Products of Ethylene Carbonate Based Electrolytes by Fourier Transform Infrared Spectroscopy. *J. Phys. Chem. C* **2014**, *118*, 14732−14738.

(6) Ryu, J. H.; Kim, J. W.; Sung, Y.-E.; Oh, S. M. Failure Modes of Silicon Powder Negative Electrode in Lithium Secondary Batteries. *Electrochem. Solid-State Lett.* **2004**, *7*, A306−A309.

(7) Kovalenko, I.; Zdyrko, B.; Magasinski, A.; Hertzberg, B.; Milicev, Z.; Burtovyy, R.; Luzinov, I.; Yushin, G. A Major Constituent of Brown Algae for Use in High-Capacity Li-Ion Batteries. *Science* **2011**, *334*, 75−79.

(8) Xun, S.; Xiang, B.; Minor, A.; Battaglia, V.; Liu, G. Conductive Polymer and Silicon Composite Secondary Particles for a High Area-Loading Negative Electrode. *J. Electrochem. Soc.* **2013**, *160*, A1380−A1383.

(9) Liu, N.; Lu, Z.; Zhao, J.; McDowell, M. T.; Lee, H.-W.; Zhao, W.; Cui, Y. A Pomegranate-inspired Nanoscale Design for Large-volume-change Lithium Battery Anodes. *Nat. Nanotechnol.* **2014**, *9*, 187−192.

(10) Obrovac, M. N.; Christensen, L.; Le, D. B.; Dahn, J. R. Alloy Design for Lithium-Ion Battery Anodes. *J. Electrochem. Soc.* **2007**, *154*, A849−A855.

(11) Song, J.; Zhou, M.; Yi, R.; Xu, T.; Gordin, M. L.; Tang, D.; Yu, Z.; Regula, M.; Wang, D. Interpenetrated Gel Polymer Binder for High-Performance Silicon Anodes in Lithium-Ion Batteries. *Adv. Functional Mater.* **2014**, *24*, 5904−5910.
(12) Liu, G.; Xun, S.; Vukmirovic, N.; Song, X.; Olalde-Velasco, P.; Zheng, H.; Battaglia, V. S.; Wang, L.; Yang, W. Polymers with Tailored Electronic Structure for High Capacity Lithium Battery Electrodes. *Adv. Mater.* **2011**, *23*, 4679−4683.
(13) Wu, M.; Xiao, X.; Vukmirovic, N.; Xun, S.; Das, P. K.; Song, X.; Olalde-Velasco, P.; Wang, D.; Weber, A. Z.; Wang, L. W.; Battaglia, V. S.; Yang, W.; Liu, G. Toward an Ideal Polymer Binder Design for High-Capacity Battery Anodes. *J. Am. Chem. Soc.* **2013**, *135*, 12048−12056.
(14) Dai, K.; Zhao, H.; Wang, Z.; Song, X.; Battaglia, V.; Liu, G. Toward High Specific Capacity and High Cycling Stability of Pure Tin Nanoparticles with Conductive Polymer Binder for Sodium Ion Batteries. *J. Power Sources* **2014**, *263*, 276−279.
(15) Zhao, H.; Wang, Z.; Lu, P.; Jiang, M.; Shi, F.; Song, X.; Zheng, Z.; Zhou, X.; Fu, Y.; Abdelbast, G.; Xiao, X.; Liu, Z.; Battaglia, V. S.; Zaghib, K.; Liu, G. Toward Practical Application of Functional Conductive Polymer Binder for a High-Energy Lithium-Ion Battery Design. *Nano Lett.* **2014**, *14*, 6704−6710.
(16) Hu, H.; Yuan, W.; Lu, L.; Zhao, H.; Jia, Z.; Baker, G. L. Low Glass Transition Temperature Polymer Electrolyte Prepared from Ionic Liquid Grafted Polyethylene Oxide. *J. Polym. Sci., Part A: Polym. Chem.* **2014**, *52*, 2104−2110.
(17) Hu, H.; Yuan, W.; Zhao, H.; Baker, G. L. A Novel Polymer Gel Electrolyte: Direct Polymerization of Ionic Liquid From Surface of Silica Nanoparticles. *J. Polym. Sci., Part A: Polym. Chem.* **2014**, *52*, 121−127.
(18) Dai, Y.; Cai, L.; White, R. E. Capacity Fade Model for Spinel $LiMn_2O_4$ Electrode. *J. Electrochem. Soc.* **2013**, *160*, A182−A190.
(19) Jia, Z.; Yuan, W.; Zhao, H.; hu, h.; Baker, G. L. Composite Electrolytes Comprised of Poly(Ethylene Oxide) and Silica Nanoparticles with Grafted Poly(ethylene oxide)-Containing Polymers. *RSC Adv.* **2014**, *4*, 41087−41098.
(20) Yuan, W.; Zhao, H.; Hu, H.; Wang, S.; Baker, G. L. Synthesis and Characterization of the Hole-Conducting Silica/Polymer Nanocomposites and Application in Solid-State Dye-Sensitized Solar Cell. *ACS Appl. Mater. Interfaces* **2013**, *5*, 4155−4161.
(21) Yuan, W.; Zhao, H.; Baker, G. L. Low Glass Transition Temperature Hole Transport Material in Enhanced-Performance Solid-State Dye-Sensitized Solar Cell. *Org. Electron.* **2014**, *15*, 3362−3369.
(22) Zheng, H.; Tan, L.; Liu, G.; Song, X.; Battaglia, V. S. Calendering Effects on The Physical and Electrochemical Properties of $Li[Ni_{1/3}Mn_{1/3}Co_{1/3}]O_2$ cathode. *J. Power Sources* **2012**, *208*, 52−57.
(23) Qin, J.; Zhao, H.; Liu, X.; Zhang, X.; Gu, Y. Double Phase Separation in Preparing Polyimide/Silica Hybrid Films by Sol−Gel Method. *Polymer* **2007**, *48*, 3379−3383.
(24) Qin, J.; Zhao, H.; Zhu, R.; Zhang, X.; Gu, Y. Effect of Chemical Interaction on Morphology and Mechanical Properties of CPI-OH/SiO_2 Hybrid Films With Coupling Agent. *J. Appl. Polym. Sci.* **2007**, *104*, 3530−3538.
(25) Striebel, K. A.; Sierra, A.; Shim, J.; Wang, C. W.; Sastry, A. M. The Effect of Compression on Natural Graphite Anode Performance and Matrix Conductivity. *J. Power Sources* **2004**, *134*, 241−251.
(26) Du, Z.; Dunlap, R. A.; Obrovac, M. N. High Energy Density Calendered Si Alloy/Graphite Anodes. *J. Electrochem. Soc.* **2014**, *161*, A1698−A1705.
(27) Dai, Y.; Cai, L.; White, R. E. Simulation And Analysis of Stress in a Li-ion Battery With a Blended $LiMn_2O_4$ and $LiNi_{0.8}Co_{0.15}Al_{0.05}O_2$ Cathode. *J. Power Sources* **2014**, *247*, 365−376.
(28) Dai, Y.; Cai, L.; White, R. E. Simulation and Analysis of Inhomogeneous Degradation in Large Format LiMn2O4/Carbon Cells. *J. Electrochem. Soc.* **2014**, *161*, E3348−E3356.
(29) Zhao, H.; Park, S.-J.; Shi, F.; Fu, Y.; Battaglia, V.; Ross, P. N.; Liu, G. Propylene Carbonate (PC)-Based Electrolytes with High Coulombic Efficiency for Lithium-Ion Batteries. *J. Electrochem. Soc.* **2014**, *161*, A194−A200.
(30) Chang, W.-S.; Park, C.-M.; Kim, J.-H.; Kim, Y.-U.; Jeong, G.; Sohn, H.-J. Quartz (SiO_2): A New Energy Storage Anode Material for Li-ion Batteries. *Energy Environ. Sci.* **2012**, *5*, 6895−6899.
(31) Jeong, G.; Lee, S. M.; Choi, N. S.; Kim, Y.-U.; Lee, C. K. Stabilizing Dimensional Changes in Si-based Composite Electrodes by Controlling The Electrode Porosity: An in Situ Electrochemical Dilatometric Study. *Electrochim. Acta* **2011**, *56*, 5095−5101.
(32) Idota, Y.; Kubota, T.; Matsufuji, A.; Maekawa, Y.; Miyasaka, T. Tin-Based Amorphous Oxide: A High-Capacity Lithium-Ion-Storage Material. *Science* **1997**, *276*, 1395−1397.
(33) Wang, C.; Wu, H.; Chen, Z.; McDowell, M. T.; Cui, Y.; Bao, Z. Self-Healing Chemistry Enables The Stable Operation of Silicon Microparticle Anodes for High-Energy Lithium-Ion Batteries. *Nat. Chem.* **2013**, *5*, 1042−1048.